NANOCOMPOSITES BASED ON POLYPROPYLENE WITH NANOSILVER PARTICLES AND ANTIBACTERIAL BEHAVIOR – A REVIEW

W. L. Oliani [1], D. F. Parra [1], L. G. H. Komatsu [1], N. Lincopan [2,3], V. K. Rangari [4], A. B. Lugao [1]

[1] Nuclear and Energy Research Institute, IPEN-CNEN/SP, Av. Prof. Lineu Prestes, 2242 – Cidade Universitária - CEP 05508-000, São Paulo, Brazil
washoliani@usp.br

[2] Department of Microbiology Institute of Biomedical Sciences, USP
[3] Department of Clinical Analysis School of Pharmacy, USP, São Paulo, Brazil
[4] Department of Materials Science and Engineering Tuskegee University, USA.

ABSTRACT

This paper presents a study of polypropylene (PP) films modified by gamma irradiation with insertion of silver nanoparticles (AgNPs) and montmorillonite (MMT) aiming bactericide effect. The use of silver (Ag) gives important antibacterial property since silver is highly toxic for bacteria. The PP matrix was processed in a twin screw extruder and polypropylene nanocomposites (PPNC) were obtained in different concentrations of 0.25%; 0.5%; 1.0%; 2.0% and 4.0% in wt% and 1% of MMT. The material was characterized by scanning electron microscopy (SEM), energy dispersive spectroscopy (EDS), field emission scanning electron microscopy (FESEM), X-ray diffraction spectroscopy (XRD), cytotoxicity assay and reduction colony-forming-unit (CFU). The analyzed films showed spherical clusters and homogeneous regions with good distribution of the silver nanoparticles. Furthermore, the PP@AgNPs films exhibited a strong antibacterial efficiency against *S. aureus*, *E. coli* and *P. aeruginosa* due to the presence of the biocidal silver nanoparticles.

Keywords: polypropylene, silver, montmorillonite, gamma irradiation, antibacterial

INTRODUCTION

Isotactic polypropylene (iPP) has many desirable physical properties such as good resistance to chemicals, high stiffness, high service temperature, and reasonable temperature stability compared to other polyolefins [1,2] and low cost[3]. However, the lack of melt elasticity strain hardening behavior has limited

its applications in extrusion foaming, extrusion coating, blow molding, and thermoforming where the extensional viscosity dominates [1,2].

Research conducted in IPEN developed the production of branched PP, based on the grafting of long-chain-branches on to PP backbone using acetylene as a crosslinker under gamma radiation process. The resulting grafting reactions occurred with rearrangement of the radicals formed in the polymer [4,5] and the main characteristic is the property of melt strength, defined as the resistance of a melt to draw-down, of great importance to all processing technologies where elongational flows and stretching of polymer melt are necessary. This material is applied to optimize foam extrusion, coating extrusion, blow molding and fiber spinning [6]. Branching effects answer to crosslinking efficiency in two opposing directions. One effect is suppressing the crosslinking due to the presence of tertiary carbon and another is enhancing the crosslinking due to increased molecular mobility [7].

Antimicrobial surfaces have applications in a range of infrastructures including hospitals, childcare centers, nursing homes, etc., to assist in minimizing the spread of disease and reducing the prevalence of illness. Hospital-acquired-infection cases have been increasing rapidly in recent decades, and the prevalence of antibiotic-resistant pathogens is one fact of particular concern due to difficulties in treating these patients [8]. The antibacterial action of silver is utilized in numerous consumer products and medical devices [9]. Active antimicrobial food packaging systems are supposed not only to passively protect food against environmental factors, but also to inhibit or retard microbial growth on food surfaces, extending food shelf life. Nanostructured antimicrobials have a higher surface area-to-volume ratio when compared with their higher scale counterparts [10].

Silver, can be extremely toxic to bacteria at exceptionally low concentrations. Owing to biocidal activity, nanosilver, have been widely used as antimicrobial agent in a multitude of application related with healthcare, food packaging systems and the industry in general. One route important to further extend the antimicrobial applications of AgNPs is the incorporation as nanoparticles into polymer matrices [11].

While there is evidence that silver nanoparticles can directly damage bacteria cell membranes, silver nanomaterials appear to exert bactericidal

activity predominantly through release of silver ions followed by increased membrane permeability, loss of the proton motive force, inducing de-energization of the cells and efflux of phosphate, leakage of cellular content, and disruption DNA replication, according literature [12].

In recent research with medical devices development [13], silver nanofibers (Nfbs) were synthesized by hydrothermal treatment the nanofibers (3 and 5 wt%) and added in the initial feed together with the catalytic system polymerizations in an ethylene atmosphere were performed, yielding PE-Ag-Nfbs-nanocomposites.

Many research report the application of silver nanoparticles prepared by reduction of silver ions intercalated into montmorillonite (MMT) with borohydride[14] and formaldehyde [15] or n-hexanol [16] and deposited on the external surface of the MMT particles with the aim biocide activity.

New class of the nanohybrid, synthesized via silver nitrate reduction in the presence of silicate clay, exhibit a high potency against bacterial growth. The plate-like clay, due to its anionic surface charges and a large surface area, serves as the support for the formation of silver nanoparticles (AgNPs) 30 nm in diameter. The thin silicate plates provide a surface for immobilizing AgNPs in one highly concentrated area but prevent them from entering the cell membrane. Subsequent cytotoxicity studies indicated that surface contact with the reduced AgNPs on clay is sufficient to initiate cell death. This toxicity is related to a loss in membrane integrity due to reactive oxygen species (ROS) generation. The hybridization of AgNPs on clay surface is viable for generating a new class of nanohybrid exhibiting mild cytotoxicity but high efficacy for battling drug-resistant bacteria [17].

Several polymeric materials with different molecular weight such as polyethylene glycol (PEG), polyvinyl alcohol (PVA), poly(N-vinyl-2-pyrrolidone) (PVP), and others, mainly water soluble, have been used as coatings of silver nanoparticles to enable particle dispersion [18], and silver nanoparticles stabilized with oleic acid (AO) [19] showed clear advantages in antibacterial activity, penetration bacteria cells, cytotoxicity, time effectiveness, efficiency, and stability against light [20].

The processing by extrusion of polyolefin (polyethylene and polypropylene) nanocomposites with acquisition of properties and biocide activity should be an economically viable method and is being researched [21-23].

The aim of the present review is to show our expertise in research of polypropylene/silver/clay nanocomposites films designed to have antimicrobial activities, with a special focus on silver metal nanoparticles and their mechanisms.

MATERIALS AND METHODS

MATERIALS

The iPP with Melt Flow Index (MFI = 1.5 dg min^{-1}) and M*w* = 338,000 g mol^{-1} from Braskem – Brazil, was supplied in pellets. Acetylene 99.8% supplied by White Martins. AgNPs was purchased from Sigma Aldrich. The PVP/K90 (average molecular weight = 1,300,000 g mol^{-1}), was purchased from Plasdone. The clay mineral used was the montmorillonite, Cloisite 20®, group of smectites, organically modified with a salt of alkyl quaternary ammonium, from BYK Additives Company and antioxidant Irganox B 215ED was provided by BASF.

METHODS

Radiation process

The irradiation process of the polymer pellets in plastic container was carried at room temperature and at dose rate of 5 kGy h^{-1}, using a multipurpose ^{60}Co gamma irradiator. The polypropylene irradiation was performed at 12.5 kGy dose monitored by a Harwell Red Perspex 4034 dosimeter. After irradiation, the samples were heated for 1 hour at 90 °C to promote the recombination and annihilation of residual radicals [24].

Preparation of the Nanocomposites

The blend of iPP and PP 12.5 kGy (50/50 wt%) were mixed with Irganox B 215 ED in a rotary mixer for 24 hours. The PPNC were prepared by addition of AgNPs at different concentrations of 0.1%; 0.25%; 0.5%; 1.0%; 1.0% (PVP), 2.0% and 4.0% in wt%. The PPNC mixture was processed in a twin-screw extruder (Haake co-rotating, Model Rheomex PTW 16/25), with the following processing conditions: the temperature profile (feed to die) was 180 to 200 °C, with a speed of 100 rpm, Fig.1. After mixing, the nanocomposites were

granulated in a granulator Primotécnica W-702-3. The PP/MMT-AgNPs films were produced in planar sheet extruder and the material was placed directly into the hopper of the extruder with a temperature profile (feed to die) of 175-210 ºC, screw speed of 20 rpm and torque of 33-45 Nm. The films were produced with a thickness of ~ 0.05 mm.

Fig.1 - Polypropylene nanocomposite blend in the extruder with spaghetti training "masterbathes" (A); Haake film blowing unit used to prepare the blown films (B); The blown film take-off transports the extruded film in an upward direction. The film is guided up to the nip rolls where the tube is flattened to create a “lay-flat” tube of film (C).

Characterization

Scanning electron microscopy and Energy dispersive spectroscopy

Specimens were examined with a Hitachi TM 3000, coupled with a Bruker Quantax 70 for the collection of EDS data. SEM coupled with backscattered electron detector (BSE) and energy dispersive X-ray spectroscopy (EDS). Sample sections for the EDS analysis were taken at 15 keV, and the acquisition period was 120 s.

Field emission scanning electron microscopy

The samples were analyzed by scanning electron microscopy with field emission, JEOL FESEM, JSM-6701F, Japan, using the accelerating voltage of 5.0 kVA which allows the observation with more resolution than conventional SEM.

X-ray diffraction spectroscopy (XRD)

X-rays diffraction (XRD) measurements were carried out in the reflection mode on a Rigaku diffractometer Mini Flex II (Tokyo, Japan) operated at 30 kV voltage and a current of 15 mA with CuKα radiation (λ = 1.541841 Å).

Cytotoxicity test

The cytotoxicity assay, according to ISO 10993-5:2009 [25], was carried out with the exposure of NCTCL929 cell cultured in a 96 wells microplate to the extract obtained by the immersion of samples in cell culture medium, MEM (minimum Eagle's medium, Sigma Co., São Paulo, Brazil), for 24 h at 37 ºC in a CO_2 humidified incubator. After this period, the medium was discarded and replaced with 0.2 mL of serially diluted extract of each sample (50; 25; 12.5; 6.25 %). The cell line was acquired from American Type Culture Collection (ATCC) bank. The cytotoxic effect was evaluated by neutral red uptake (NRU) methodology [26] adapted according to previous work [27].Negative control used was non-toxic PVC pellets and positive control used was 0.02 % phenol solution. Positive and negative controls were necessary to confirm the performance of the assay. Negative results imply in no cytotoxicity effect on human cells.

Reduction colony-forming-unit (CFU)

The antimicrobial activity and efficacy were evaluated according to adaptation of the standard JIS Z 2801: 2010 [28]. Each of the micro-organisms used was activated to the respective stock cultures in appropriate culture medium to obtain inoculate. The cell suspension obtained was tested for each phase standardized in order to obtain an inoculum concentration of $900x10^6$ CFU mL^{-1}. The procedure was performed separately for each culture/sample to be tested: 100 mL of inoculum suspension was placed on the specimen, previously sterilized with 70 % alcohol, spreading over an area corresponding to $40x40mm^2$. It was incubated in Petri dishes, for approximately 24 h at 37 ºC. After the incubation time, three dilutions were done to facilitate counting of the colonies. Later, another four dilutions were performed, 10x, 100x, 1000x, and 10000x, respectively. Each dilution was carried out using agar petri plate containing PDA and incubated at 37 ºC for 24 h. The percentage reduction in

bacterial growth was calculated from the number of surviving bacteria in the petri dish after incubation for 24 h at 37 ºC, multiplied by the dilution.

RESULTS AND DISCUSSIONS

Scanning Electron Microscopy and Energy Dispersive Spectroscopy

The degree of dispersion of nanofillers plays an important role in influencing the properties of the resulting nanocomposites and energy dispersive X-ray spectroscopy (EDX), combined with scanning electron microscopy, was employed to analyse the elemental composition on the surface and following through the bulk of the sample, Fig. 2.

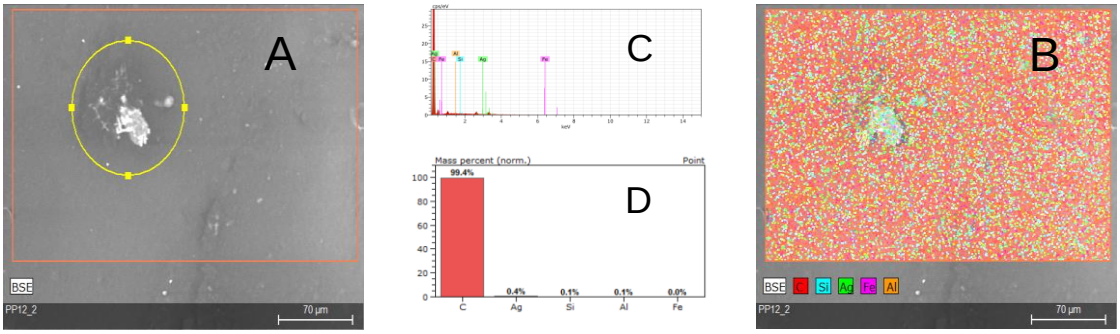

Fig.2 - Elemental maps (scale= 70μm) from SEM–EDS micrographs of PP-AgNPs-MMT film .(A); Surface of the PP–0.5% AgNPs and clay nanocomposite film shows the distribution of carbon (red), silver (green), silicon (blue), iron (purple) and aluminum (orange) (B); EDS spectrum of the PP nanocomposite film (C); Mass percent (%) of the elements in semi-quantitative-analysis (D).

The evidence of the elemental analysis suggests that the nanofiller are well dispersed within and throughout the bulk PP matrix, supporting the observation that the blending process was thorough. It is also observed clay pellets in the polymeric matrix, as SEM micrograph and confirmed by analysis of EDS.

Field Emission Scanning Electron Microscopy

Fig.3 shows the SEM image of Ag nanoparticles composition in film of PPNC.

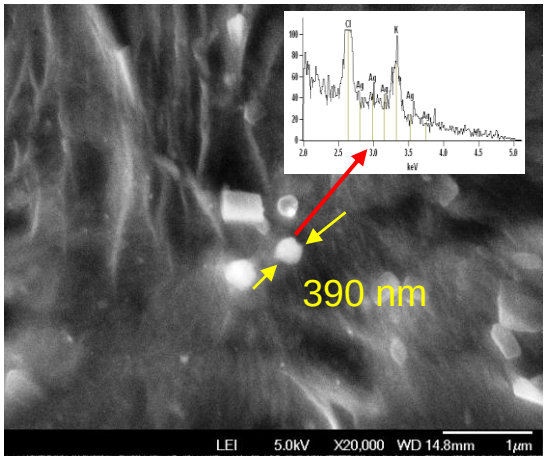

Fig.3 – FE-SEM micrograph of PPNC with silver nanoparticles.

It is observed in Fig. 3, agglomerated with the rounded shape and whose characterization by EDS is identified as silver-particles. This cluster was measured and the dimensional features around 390 nm.

X-Ray Diffraction Spectroscopy

The XRD patterns of the samples are shown in Fig. 4.

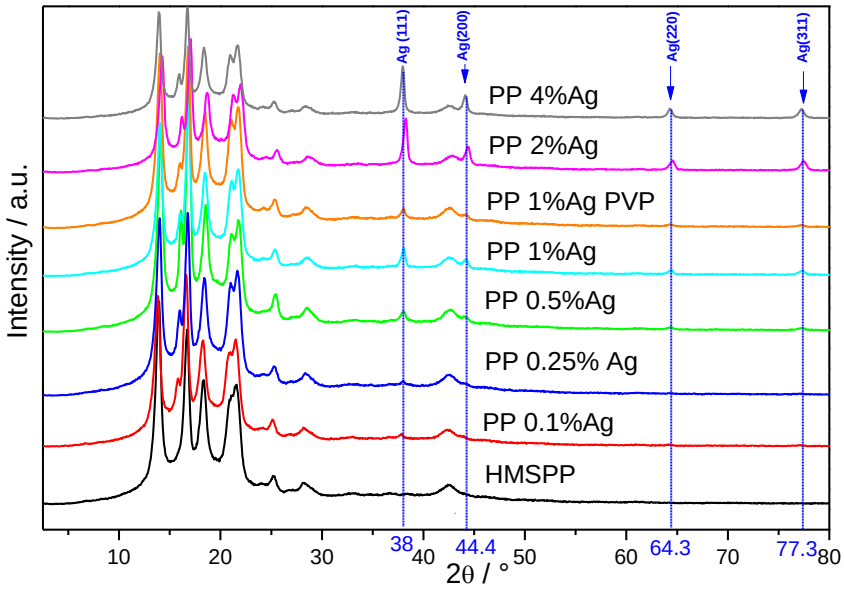

Fig. 4 – X-ray diffraction (XRD) patterns of the study samples polypropylene nanocomposite.

The XRD profile presented in Fig.4, films of PP@AgNPs, exhibit characteristic peaks at 2θ (degrees) of 38.0, 44.4, 64.3, and 77.3 corresponding to scattering from the (111), (200), (220), and (311) crystallographic planes

AgNPs. These diffraction peaks shown in Fig.4 represent a face centered cubic (fcc) structure of crystalline AgNPs and confirmed in the literature [29].

Cytotoxicity Test

In the cytotoxicity test, the PP film with AgNPs showed similar behavior to the negative control; that is, the film did not show toxicity, Fig. 5.

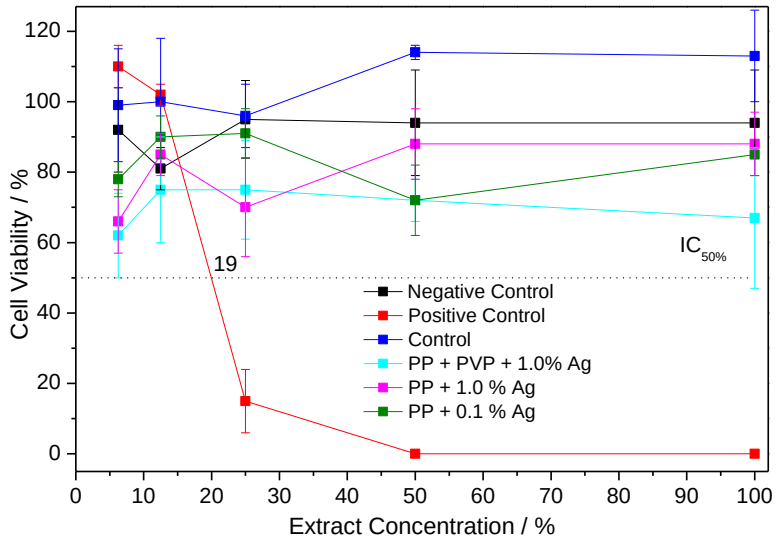

Fig. 5 - Cytotoxicity test results of Cell viability curves using neutral red uptake cytotoxicity assay, with NCTC clone 929 cells for different PP@AgNPs films.

In the cytotoxicity test, the PP film with AgNPs showed similar behavior to the negative control, the film did not show toxicity, Fig. 5. Therefore, the PP@AgNPs film was characterized as noncytotoxic for human contact.

Reduction Colony-Forming-Unit

The test of percentage reduction for CFU in the PP@AgNPs films is shown in Fig.6.

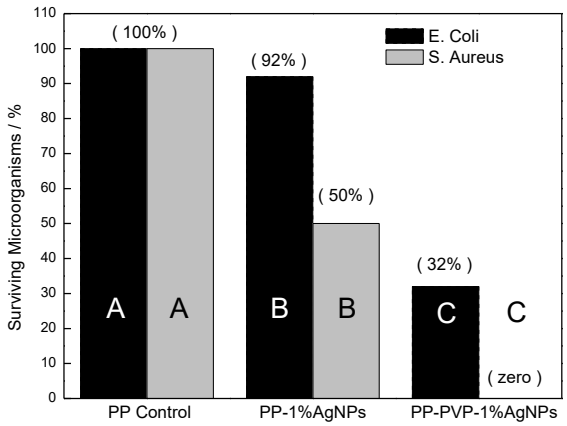

Fig.6 - Surviving microorganism percentages after 24 h of incubation for *S. aureus* and *E. coli* in the (A) PP 12.5 kGy control, (B) PP 12.5 kGy/1% AgNPs, and (C) PP 12.5 kGy/PVP 1%AgNP in films.

The test of percentage reduction for CFU in the PP@AgNPs films showed an excellent effect for *S. aureus,* Fig.6, with biocide effectiveness after 24 hours of incubation. It is also observed 68% reduction of *E. coli* of the PP@AgNPs films versus the PP film control without AgNPs assured a satisfactory antibacterial efficacy. However for the other samples cited in this work is not obtained satisfactory results i.e. the samples showed no biocide activity.

CONCLUSIONS

The addition of AgNPs to a PP matrix during the extrusion process has very important results and of interest to the industrial development of films with biocide properties by increasing the protection against *S. aureus* and *E. coli*. AgNPs in the PP film properly hindered the bacterial activity in the bulk, and when appropriated surfactants were used, the overall effect was a high antibacterial efficiency on the surface. The percentage reduction for the CFU assay showed positive biocidal results for *S. aureus* and *E. coli*. The cytotoxicity test for the PP film with AgNPs showed no cytotoxicity effects on mammalian cells.

ACKNOWLEDGEMENTS

The authors acknowledge financial support for this work from CAPES-Process: CSF-PVE’s - 88887.115684/2016-00, CCTM/IPEN, for microscopy analysis (FESEM), Sizue O. Rogero, laboratory biomaterials polymeric CQMA/IPEN, for the cytotoxicity tests and multipurpose gamma irradiation facility at the CTR/IPEN.

REFERENCES

1. PARK, C.B.; CHEUNG, L. K. A. study of cell nucleation in the extrusion of polypropylene foams. *Polym. Eng. Sci*., 37, 1-10, 1997.

2. NAGUIB, H. E.; PARK, C. B.; REICHELT, N. Fundamental foaming mechanisms governing the volume expansion of extruded polypropylene foams. *J. Appl. Polym. Sci*., 91, 2661-2668, 2004.

3. TJONG, S. C.; LI, R. K. Y.; CHEUNG, T. Mechanical behavior of $CaCO_3$ particulate filled β-crystalline phase polypropylene composites. *Polym. Eng. Sci.*, 37, 1, 166-172, 1997.

4. OLIANI, W. L.; PARRA, D. F.; LIMA, L. F. C. P.; LUGAO, A. B. Morphological characterization of branched PP under stretching. *Polym. Bull*., 68, 2121-2130, 2012.

5. OTAGURO, H.; LIMA, L. F. C. P.; PARRA, D. F.; LUGAO, A. B.; CHINELATTO, M. A.; CANEVAROLO, S. V. High-energy radiation forming chain scission and branching in polypropylene. *Radiat. Phys. Chem*., 79, 318-324, 2010.

6. LUGAO, A. B.; ARTEL, B. W. H.; YOSHIGA, A.; LIMA, L. F. C. P.; PARRA, D. F.; BUENO, J. R.; LIBERMAN, S.; FARRAH, M.; TERÇARIOL, W. R.; OTAGURO, H. Production of high melt strength polypropylene by gamma irradiation. *Radiat. Phys. Chem*., 76, 1691-1695, 2007.

7. MAKUUCHI, K.; CHENG, S. *Radiation Processing of Polymer Materials and its Industrial Applications*, John Willy & Sons, Inc., New Jersey & USA, 2012.

8. HANUS, M. J.; HARRIS, A. T. Nanotechnology innovations for the construction industry. *Prog. Mater. Sci.* 58, 1056–1102, 2013.

9. CHERNOUSOVA, S.; EPPLE, M. Silver as Antibacterial Agent: Ion, Nanoparticles, and Metal. *Angew. Chem. Int*., 52, 1636 – 1653, 2013.

10. AZEREDO, H. M. C. Antimicrobial nanostructures in food packaging. *Trends Food Sci. Tech.,* 30, 56-69, 2013.

11. PALZA, H. Antimicrobial Polymers with Metal Nanoparticles. *Int. J. Mol. Sci.*, *16*, 2099-2116, 2015.

12. MARAMBIO-JONES, C.; HOEK, E. M. V. A review of the antibacterial effects of silver nanomaterials and potential implications for human health and the environment. *J. Nanopart. Res.,* 12, 1531–1551, 2010.

13. ZAPATA, P. A.; LARREA, M.; TAMOYO, L.; RABAGLIATI, F. M.; AZÓCAR, M. I.; PÁEZ, A. Polyethylene/silver-nanofiber composites: A material for antibacterial films. *Mater. Sci. Eng. C.* 69, 1282-1289, 2016.

14. GIRASE, B.; DEPAN, D.; SHAH, J. S.; XU, W.; MISRA, R. D. K. Silver–clay nanohybrid structure for effective and diffusion-controlled antimicrobial activity. *Mater. Sci. Eng. C.,* 31, 1759–1766, 2011.

15. PRAUS, P.; TURICOVÁ, M.; MACHOVIC, V.; STUDENTOVA, S.; KLEMENTOVA, M. Characterization of silver nanoparticles deposited on montmorillonite. *Appl. Clay Sci*., 49, 341-345, 2010.

16. MIYOSHI, H.; OHNO, H.; SAKAI, K.; OKAMURA, N.; KOURAI, H. Characterization and photochemical and antibacterial properties of highly stable silver nanoparticles prepared on montmorillonite clay in n-hexanol. *J. Colloid Interface Sci.* 345, 433–441, 2010.

17. SU, H. L.; CHOU, C. C.; HUNG, D. J.; LIN, S. H.; PAO, I. C.; LIN, J. H.; HUANG, F. L.; DONG, R. X.; LIN, J. J. The disruption of bacterial membrane integrity through ROS generation induced by nanohybrids of silver and clay. *Biomaterials*. 30, 5979–5987, 2009.

18. FOLDBJERG, R.; OLESEN, P.; HOUGAARD, M.; DANG, D. A.; HOFFMANN, H. J.; AUTRUP, H. PVP coated silver nanoparticles and silver ions induce reactive oxygen species, apoptosis and necrosis in THP-1 monocytes. *Toxicol. Lett.,* 28, 190, 2, 156-162, 2009.

19. SARKAR, A.; KAPOOR, S.; MUKHERJEE, T. Oleic acid-assisted phase transfer of nanosized silver colloids. *Res. Chem. Intermed*., 36, 403–410, 2010.

20. AZOCAR, M. I.; TAMAYO, L.; VEJAR, N.; GÓMEZ, G.; ZHOU, X.; THOMPSOM, G.; CERDA, E.; KOGAN, M. J.; SALAS, E.; PAEZ, M. A. A systematic study of antibacterial silver nanoparticles: efficiency, enhanced permeability, and cytotoxic effects. *J. Nanoparticle Resear.,* 16, 2465, 2014.

21. OLIANI, W. L.; PARRA, D. F.; LIMA, L. F. C. P.; LINCOPAN, N.; LUGAO, A. B. Development of a nanocomposite of polypropylene with biocide action from silver nanoparticles. *J. Appl. Polym. Sci.*, 132, 42218, 2015.

22. FAGES, E.; FENOLLAR, O.; SANOGUERA, D. G.; BALART, R. Study of antimicrobial properties of polypropylene filled with surfactant coated silver nanoparticles *Polym. Eng. Sci.*, 51, 804, 2010.

23. SAHOO, R. K.; MOHANTY, S.; NAYAK, S. K. Effect of silver nanoparticles on the morphology, crystallization, and melting behavior of polypropylene: A study on non-isothermal crystallization kinetics. *Polym. Sci. A*., 58, 443-453, 2016.

24. OLIANI, W. L.; PARRA D. F.; LUGAO, A. B. UV stability of HMSPP (high melt strength polypropylene) obtained by radiation process. *Radiat. Phys. Chem.,* 79, 383–387, 2010.

25. ISO 10993-5:2009 – Biological evaluation of medical devices. Pat 5: Tests for in vitro cytotoxicity.

26. CIAPETTI, G.; GRANCHI, D.; VERRI, E.; SAVARINO, L.; CAVEDAGNA, D.; PIZZOFERRATO, A. Application of a neutral red and starch black staining for rapid, reliable cytotoxicity testing of biomaterials. *Biomaterials*. 17, 1259-1264, 1996.

27. ROGERO, S. O.; MALMONGE, S. M.; LUGAO, A. B.; IKEDA, T. I.; MIYAMARU, L.; CRUZ, A. S. Biocompatibility study of polymeric biomaterials. *Artif. Organs*. 27, 5, 424–427, 2003.

28. JIS Z 2801:2010 - JAPANESE industrial standard – antibacterial products - test for antibacterial activity and efficacy.

29. R. KAKKAR; E. D. SHERLY; K. MADGULA, D. K. DEVI; B. SREEDHAR. Synergetic effect of sodium citrate and starch in the synthesis of silver nanoparticles. *J. Appl. Polym. Sci.*, 126, E154-E161, 2012.